Mutual deactivation of electrically active F interstitials and O vacancies into fluorine-oxygen-vacancy complexes in SiO_2

Eun-Cheol Lee* and Heongkyu Ju
College of Bio-Nano Technology, Kyungwon University, Gyeonggi 461-701, Korea
and Gachon Bio-Nano Research Institute, Gyeonggi 461-701, Korea
(Received 16 January 2009; revised manuscript received 2 April 2009; published 6 May 2009)

Based on first-principles density-functional calculations, we show that F interstitials in SiO_2 behave as negative fixed charges or as charge traps, depending on their positions relative to the Si/SiO_2 interface. By contrast, they deactivate O vacancies, which are the dominant charge traps in SiO_2, by forming F-pair complexes at O sites, while a defect complex of an O vacancy and a F atom is still a electrically active negative-U center. Our model successfully explains the controversial points in earlier experimental analyses and suggests that a proper thermal annealing process under a moderate F doping level will lead to the improved electrical properties for SiO_2 by effectively deactivating the O vacancies and the F interstitials into the F-pair complexes.

DOI: 10.1103/PhysRevB.79.193203 PACS number(s): 61.72.−y, 71.55.−i, 77.84.Bw, 85.30.−z

The control of defects in SiO_2 is one of the critical issues in manufacturing metal-oxide-semiconductor (MOS) transistors with minimum feature sizes smaller than 100 nm. Fluorine, one of the most important extrinsic impurities in SiO_2, affects the performance of the transistors. A number of processes, including the W-related process involving WF_6 decomposition,[1,2] fluorine-based plasma etching,[3,4] and BF_2 source-drain implant,[5,6] unavoidably incorporate F into the gate oxide, and it has been shown that fluorine improves electrical properties related to the Si/SiO_2 interface, such as negative bias temperature instability (NBTI) and hot carrier immunity.[7–10] The theoretical explanation for these effects is that Si dangling bonds at the interface are effectively deactivated by fluorine atoms into Si-F bonds.[11]

The effects of fluorine incorporation into the bulk region of SiO_2 have also been extensively studied. It has been reported, for instance, that the electrical characteristics of the bulk region of SiO_2 can be improved,[12] changed very little,[7] or degraded[13] by the incorporation of F, with the results being based on analyses such as stress-induced leakage current (SILC), charge to breakdown (Q_{BD}), and oxide breakdown voltage. Although Sugizaki *et al.*[14] showed that the electrical properties of the bulk region vary, depending the F concentration, there is not yet a good understanding of the various experimental features. Moreover, an understanding of the role of fluorine at the atomic scale is necessary in order to determine the optimum growth conditions for F-doped SiO_2.

In this paper, we present an atomic model for how F is incorporated into SiO_2, based on first-principles pseudopotential calculations. We find that the F interstitials act as negative fixed charges or charge traps, while they deactivate O vacancies, which are dominant charge traps in SiO_2, by forming F-pair complexes at O sites. Thus, the electrical properties of SiO_2 are expected to be strongly dependent on the degree of mutual deactivation of F interstitials and O vacancies through the formation of the inactive F pairs. Our results are in good agreement with the previously reported experimental features and indicate the optimum conditions for obtaining high-quality SiO_2 with F impurities.

We calculate the total energies of F-related defects in SiO_2 using first-principles density-functional theory (DFT), as implemented in the VASP code,[15–18] within the generalized gradient approximation (GGA).[19] We use ultrasoft pseudopotentials[20,21] with a kinetic-energy cutoff of 430 eV and a supercell containing 72 host atoms in the α-quartz structure. The Γ point is used for sampling the Brillouin zone. For charged defects, we corrected the errors from the spurious monopole-monopole interaction between the background and defect charges;[22] these errors are estimated to be 0.5, 2.1, and 4.8 eV for singly, doubly, and triply charged states, respectively. The top of SiO_2 valence band is set as zero reference energy to describe defect levels in the SiO_2 band gap.

The first result from our investigation of the atomic and electronic structures of F interstitials (F_i) is that there are two dominant classes, $F(1)_i$ and F_O-O_i, of these interstitials. The former involves a monovalent F atom which does not break any Si-O bonds and which is bonded to a fivefold-coordinated Si atom [see Fig. 1(a)]. In the latter, the positions of the F and the O_I atoms are exchanged relative to their relationship in $F(1)_i$, resulting in the breaking of the bond

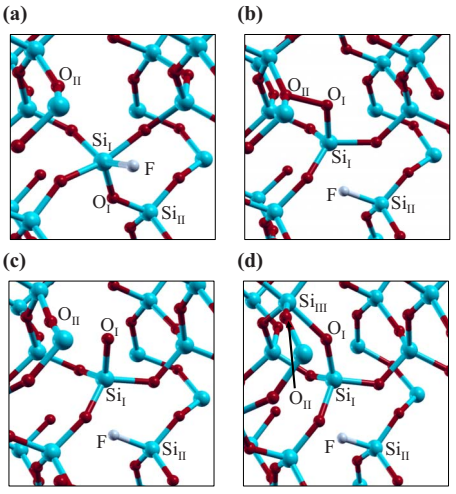

FIG. 1. (Color online) (a) Atomic structure of $F(1)_i$ for the neutral charge state. The atomic structures of F_O-O_i are shown for the (b) 1+, (c) neutral, and (d) 1− charge states.

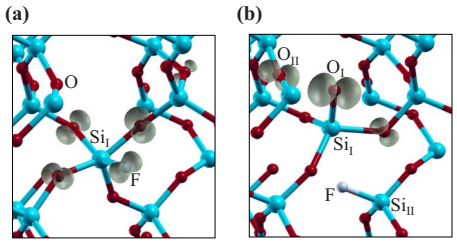

FIG. 2. (Color online) Charge densities for the half-filled defect levels of the neutral (a) $F(1)_i$ and (b) F_O-O_i defects for an isosurface of 0.015 a.u.

between the O_I and the Si_{II} atoms. As shown in Figs. 1(b)–1(d), the local bonding configurations around the O_I atom are different for the 1+, neutral, and 1− charge states. $F(1)_i$ has a half-filled defect level at 0.30 eV, which is characterized by a $pp\sigma^*$ coupling between the F atom and the neighboring O atoms [see Fig. 2(a)]. In contrast to the situation with F_O-O_i, the structures of $F(1)_i$ in the negatively and positively charged states are similar to the structure in the neutral state.

The stable geometries of F_O-O_i are different for the different charge states, as noted above. In the case of the neutral charge state, the O_I atom is only bonded to the Si_I atom, forming a nonbridging Si_I-O_I radical [Fig. 1(c)], while the lowest energy configuration O_i in SiO_2 is a peroxy linkage structure with the O interstitial incorporated in the Si-O-Si bond.[23,24] We find that the F_O-O_i complex has a binding energy of 4.00 eV against dissociation to F_O and a remote interstitial O. This complex has defects levels at 0.56 and 1.30 eV, which are characterized, respectively, by $pp\pi^*$ and $pp\sigma^*$ interactions between the O_I and neighboring O atoms. The higher $pp\sigma^*$, which is shown in Fig. 2(b), is half filled in the neutral charge state. The fact that the $pp\sigma^*$ level in the 1− charge state is fully occupied leads to a stronger repulsion between the O_I and O_{II} atoms and the relaxation of these two O atoms creates an additional Si_{III}-O_I bond, as shown in Fig. 1(d). For the 1+, 2+, and 3+ states, where the $pp\pi^*$ level is empty, an O_I-O_{II} bond is formed because the repulsion between these two O atoms is mostly reduced [Fig. 1(b)].

Based on the formation energies of the F interstitials in Fig. 3, $F(1)_i^-$ is found to be stable for the wide range of Fermi levels above 1.62 eV. $F(1)_i^-$ and $(F_O$-$O_i)^-$ are stabilized for all Fermi levels at 1.32–1.62 and at 0–1.32 eV, respectively. We align the experimental Si band gap with our SiO_2 band gap using the position of the Si band estimated by Blöchl and Stathis;[25] the defect level of atomic hydrogen was shown to be at 0.2 eV above the Si midgap.[26] Together with the measured Si band gap (1.1 eV) and the calculated H level in the DFT band gap of SiO_2 (4.1 eV), this finding determines the Si band gap to be at 3.3–4.4 eV in the DFT band gap of SiO_2,[25] as depicted in Fig. 3. Since, under thermal equilibrium conditions, the Fermi level of SiO_2 should lie within the Si band gap (the shaded region in Fig. 3), $F(1)_i^-$ is expected to be the most abundant F interstitial. We check if our conclusions are affected by the higher-order errors of the charged supercells vanishing as $1/L^3$,[22] where L is the linear dimension of the supercell. The test calculations are performed in a 576-atom cell, which is generated by doubling

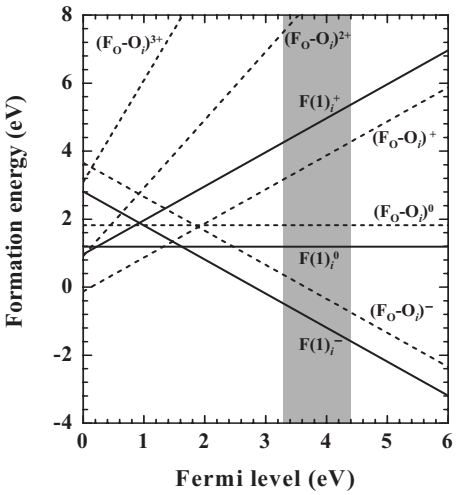

FIG. 3. Formation energies of F interstitials as a function of the Fermi level. Shaded region indicates the band gap of Si aligned to that of SiO_2.

the lattice constants of the 72-atom cell, for two dominant F-related defects around the interface, i.e., $F(1)_i^-$ and $(F_O$-$O_i)^-$. It is found that the formation energies of the defects slightly increase by the same amount of 30 meV and thus the relative energy difference remains unchanged within 1 meV. Therefore, the monopole corrections used here are sufficiently accurate to draw our results.

The defect transition levels indicate that an F interstitial acts as a negative fixed charge near the Si/SiO_2 interface. The defect transition level between two different charge states is at the Fermi level where the defect formation energy curves for the two charge states intersect. As shown in Fig. 3, the $(1+/0)$ and $(0/1-)$ transition levels for $F(1)_i$ lie at 0.23 and 1.62 eV, respectively. Similar to the case discussed above, $F(1)_i$ should be in the 1− charge state in the equilibrium states because the $(0/1-)$ level is below the Si band gap. At the interface or its adjacent region, because of free exchange of excess or deficient electrons with the adjacent Si, $F(1)_i$ can maintain the 1− charge state even for nonequilibrium charge injections. Thus, we suggest that $F(1)_i$ at the interface is the origin of the F-induced negative fixed charge that has been observed in experiments.[27] This negative fixed charge can shift the threshold voltage and degrade the carrier mobility through the Coulomb scattering, which degrades the performance of a MOS device. Away from the interface, $F(1)_i$ behaves like a charge trap instead of a negative fixed charge because it cannot freely exchange charges with Si. Since the $(1+/0)$ and $(0/1-)$ transition levels are closer to the valence-band maximum (VBM) of SiO_2 (see Fig. 3), $F(1)_i$ easily captures electrons and thus may act as a electron trap over a wide range of the Fermi level, explaining the F-induced electron traps observed in experiments.[28] When a gate bias is applied high enough to make the defect appear between the Fermi levels of the anode and cathode, trap-assisted electron tunneling can occur through this defect, which leads to a gate leakage current. We find that the $(1+/1-)$ transition level for F_O-O_i is at 1.89 eV. F_O-O_i acts as a negative fixed charge or a charge trap just as $F(1)_i$ does, but it is less stable than $F(1)_i$ under the equilibrium growth

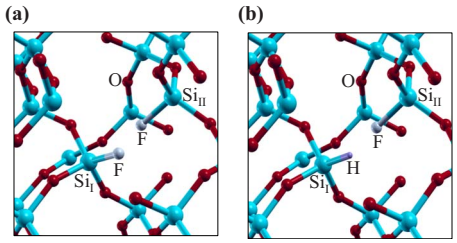

FIG. 4. (Color online) Atomic structures of the (a) $(F_2)_O$ and (b) F_i-H_O complexes.

condition where the Fermi level lies within the Si band-gap region. We note that our calculations with the crystalline quartz supercell do not take into account the disorder of atomic positions in the amorphous phase. Since amorphous SiO_2 has a local atomic ordering that is very similar to that of α quartz, our results based on the α-quartz structure may also remain valid in most regions of the amorphous matrix. However, we cannot rule out the possibility that, in some regions with large disorder-induced strain, $(F_O\text{-}O_i)^-$ is locally more stabilized than $F(1)_i^-$ because $(F_O\text{-}O_i)^-$ can effectively reduce the strain by breaking the strained Si-O bond [see the Si_{II}-O_I bond rupture in Fig. 1(d)].

On the other hand, F interstitials also improve the electrical properties of SiO_2. It was reported that, at the interface, a single F interstitial is effective for deactivating the interface trap with one Si dangling bond.[11] However, we find that a single F interstitial cannot passivate the dominant charge trap in the bulk region, i.e., an O vacancy (V_O); instead, a defect complex of an O vacancy and a F atom (F_O) is a negative-U defect with the $(1+/1-)$ transition level at 4.44 eV. We do find, however, that a pair of F interstitials at an O site $[(F_2)_O]$, as shown in Fig. 4(a), effectively removes the electrical activity of the O vacancy without leaving any defect level in the SiO_2 band gap. $(F_2)_O$ is energetically very stable because the reaction $2F(1)_i + V_O \rightarrow (F_2)_O$ is exothermic by 9.42 eV. For $(F_2)_O$, the adsorption energy of one F atom on the O vacancy is 4.71 eV, which is 1.84 eV higher than for F_O, because two F atoms share the energy cost of breaking the dimerized Si-Si bond in the O vacancy. Thus, two F interstitials energetically prefer to be adsorbed on the same O vacancy, forming the $(F_2)_O$ defect, rather than being adsorbed on two different O vacancies.

We also calculate the vibration frequency of the F-Si stretch mode for $(F_2)_O$ which is 840 cm^{-1}. This is about 10.6% lower than the 940 cm^{-1} peak from infrared adsorption spectroscopy measurements on F-doped silica glasses.[29–31] Since errors of about 10% in the calculations of vibration frequencies are not unusual,[32] we suggest that $(F_2)_O$-like defects are responsible for the peak at 940 cm^{-1}. For $F(1)_i^-$, it is found that the vibrational frequency is 706 cm^{-1}, lower than that of $(F_2)_O$; the reason for the difference is that, for $F(1)_i^-$, the F atom is bonded to the overcoordinated Si atom, as shown in Fig. 1(a), which results in a weaker Si-F bond. This peak did not appear clearly in experiments,[29–31] but this might be due to the fact that the concentrations of $F(1)_i^-$ were not high enough for the relevant peaks to be visible against other strong peaks in this wave-number range. Evidence for this explanation comes from the fact that even 940 cm^{-1} peaks were not detected in F-incorporated SiO_2 gate dielectrics grown by oxidation,[33,34] where the F concentrations are much lower than those in F-doped silica glasses.

On the other hand, a single F interstitial can deactivate a H atom at an O site (H_O) which is responsible for the stress-induced leakage current;[25] as shown in Fig. 4(b), H_O is deactivated into a F_i-H_O complex with an exothermic reaction energy of 6.33 eV.

The combination of the positive and negative effects of F can explain why different experiments observe the improved, almost unchanged, or degraded electrical characteristics after the introduction of F. The electrical properties may strongly depend on the degree of mutual deactivation of electrically active F interstitials and O vacancies as they form the inactive F pairs. Our results can provide optimum conditions to improve the electrical properties of SiO_2 with F incorporated. The first requirement is to maintain the F concentration within a moderate range, as previously reported.[14] If the concentration of F is much lower than that of the O vacancies, the effect of deactivating O vacancies can be negligible. Excessive F incorporation is similarly unfavorable for the electrical properties because any extra fluorine interstitials after the O vacancies have been deactivated will act as fixed charges or charge traps. We note, however, that a moderate doping level of F does not guarantee electrical improvement. The nonequilibrium F interstitials can be frozen in metastable states, whereas the deactivation of O vacancies caused by F pairing is energetically favorable. Thus, the second step in maximizing the electrical improvement is to include a suitable thermal annealing process if the concentration of F defects incorporated through nonequilibrium processes is high. Finally, we suggest that, in addition to differences in the F concentration, another cause for the diversity in the experimental results be the various thermal budgets after F incorporation.

In conclusion, we find that fluorine has both a beneficial and an adverse effect on the electrical properties of SiO_2. F interstitials act as negative fixed charges or charge traps, while the dominant charge traps such as O vacancies and H-bridge defects can be deactivated via the formation of $(F_2)_O$ and F_i-H_O, respectively. Thus, the competition between these positive and negative effects may determine the electrical properties, leading to the different oxide qualities, in good agreement with experiments. We suggest that, in a MOS process, the F concentration and the thermal budget after the incorporation of F play a key role in obtaining electrically optimized SiO_2.

This research was supported by the GRRC program of Gyeonggi province (Grant No. 2008-0166) and the Kyungwon University Research Fund in 2007. All figures were generated by XCRYSDEN program (Ref. 35).

*Corresponding author; eclee@kyungwon.ac.kr

[1] H. J. Whitlow, T. Eriksson, M. Östling, C. S. Petersson, J. Keinonen, and A. Anttila, Appl. Phys. Lett. **50**, 1497 (1987).
[2] K.-C. Huang, Y.-K. Fang, D.-N. Yaung, J.-C. Hseih, and M.-S. Liang, Jpn. J. Appl. Phys., Part 2 **38**, L1091 (1999).
[3] D. L. Flamm, V. M. Donnelly, and J. A. Mucha, J. Appl. Phys. **52**, 3633 (1981).
[4] B. W. Smith, C. Fonseca, L. Zavyalova, Z. Alam, and A. Bourov, J. Vac. Sci. Technol. B **15**, 2259 (1997).
[5] M. Delfino and M. E. Lunnon, J. Electrochem. Soc. **132**, 435 (1985).
[6] S. Wolf, *Silicon Processing for the VLSI Era* (Lattice, Sunset Beach, CA, 1990), Vol. 2.
[7] T. B. Hook, E. Adler, F. Guarin, J. Lukaitis, N. Rovedo, and K. Schruefer, IEEE Trans. Electron Devices **48**, 1346 (2001).
[8] D. K. Schroder and J. A. Boncock, J. Appl. Phys. **94**, 1 (2003).
[9] P. J. Wright and K. C. Saraswat, IEEE Trans. Electron Devices **36**, 879 (1989).
[10] Y. Nishioka, E. F. D. Silva, Y. Wang, and T.-P. Ma, IEEE Electron Device Lett. **9**, 38 (1988).
[11] L. Tsetseris, X. J. Zhou, D. M. Fleetwood, R. D. Schrimpf, and S. T. Pantelides, Appl. Phys. Lett. **85**, 4950 (2004).
[12] P. Chowdhury, A. I. Chou, K. Kumar, C. Lin, and J. C. Lee, Appl. Phys. Lett. **70**, 37 (1997).
[13] T. Nakanishi, T. Kawamoto, and K. Takasaki, Jpn. J. Appl. Phys., Part 1 **37**, 4316 (1998).
[14] T. Sugizaki, A. Murakoshi, Y. Ozawa, T. Nakanishi, and K. Sugura, Jpn. J. Appl. Phys., Part 1 **40**, 2674 (2001).
[15] G. Kresse and J. Hafner, Phys. Rev. B **47**, 558 (1993).
[16] G. Kresse and J. Hafner, Phys. Rev. B **49**, 14251 (1994).
[17] G. Kresse and J. Furthmuller, Comput. Mat. Sci. **6**, 15 (1996).
[18] G. Kresse and J. Furthmuller, Phys. Rev. B **54**, 11169 (1996).
[19] J. P. Perdew, in *Electronic Structure of Solids*, edited by P. Ziesche and H. Eschrig (Akademie-Verlag, Berlin, 1991).
[20] D. Vanderbilt, Phys. Rev. B **41**, 7892 (1990).
[21] G. Kresse and J. Hafner, J. Phys.: Condens. Matter **6**, 8245 (1994).
[22] G. Makov and M. C. Payne, Phys. Rev. B **51**, 4014 (1995).
[23] D. R. Hamann, Phys. Rev. Lett. **81**, 3447 (1998).
[24] G. Pacchioni and G. Ieranò, Phys. Rev. B **56**, 7304 (1997).
[25] P. E. Blöchl and J. H. Stathis, Phys. Rev. Lett. **83**, 372 (1999).
[26] R. E. Stahlbush, E. Cartier, and D. A. Buchanan, Microelectron. Eng. **28**, 15 (1995).
[27] Y. Suizu, IEEE Trans. Electron Devices **48**, 2777 (2001).
[28] L. Vishnubhotla, T. P. Ma, H.-H. Tseng, and P. J. Tobin, Appl. Phys. Lett. **59**, 3595 (1991).
[29] K. Saito and A. J. Ikushima, J. Appl. Phys. **91**, 4886 (2002).
[30] S.-J. Ding, L. Chen, X.-G. Wan, P.-F. Wang, J.-Y. Zhang, D. W. Zhang, and J.-T. Wang, Mater. Chem. Phys. **71**, 125 (2001).
[31] H. Hosono, M. Mizuguchi, and L. Skuja, Opt. Lett. **24**, 1549 (1999).
[32] Y.-S. Kim, Y.-G. Jin, J.-W. Jeong, and K. J. Chang, Semicond. Sci. Technol. **14**, 1042 (1999).
[33] Y. Mitani, H. Satake, Y. Nakasaki, and A. Toriumi, IEEE Trans. Electron Devices **50**, 2221 (2003).
[34] T. P. Ma, J. Vac. Sci. Technol. A **10**, 705 (1992).
[35] A. Kokalj, Comput. Mater. Sci. **28**, 155 (2003); Code available from http://www.xcrysden.org/